Available online at www.sciencedirect.com
SciVerse ScienceDirect
ELSEVIER
Ceramics International 38 (2012) 2693–2699
CERAMICS INTERNATIONAL
www.elsevier.com/locate/ceramint

Electromagnetic wave absorption by an organic resin solution based on ferrite particles with a spinel crystal structure

Branka Mušič [a,*], Miha Drofenik [c,d], Peter Venturini [a], Andrej Žnidaršič [b,c]

[a] Helios Domžale d.d., Količevo 2, 1230 Domžale, Slovenia[1]
[b] Nanotesla Institut, Stegne 29, 1521 Ljubljana, Slovenia
[c] Centre of Excellence NAMASTE, Slovenia
[d] Faculty of Chemistry and Chemical Engineering, Smetanova ulica 17, 2000 Maribor, Slovenia

Received 6 July 2011; received in revised form 11 November 2011; accepted 14 November 2011
Available online 20 November 2011

Abstract

We have investigated an organic resin solution designed for EM wave absorption based on a magnetic filler, composed of phases within the $Mn_{0.66}Zn_{0.27}Fe_{2.07}O_4$ system, embedded in an absorber composite with concentration ratios of 50:50, 75:25 and 90:10 by weight. The formation of the manganese zinc ferrite particles, as the principal magnetic phases, was achieved via the conventional ceramic method. The electromagnetic parameters of the composites were measured with a vector network analyser at 100 MHz to 10 GHz. The subject of the paper was a study of the electromagnetic absorber properties and the rheological properties of the resin composite based on ferrite particles with respect to using the materials in architectural coatings.
© 2011 Elsevier Ltd and Techna Group S.r.l. All rights reserved.

Keywords: D. Ferrites; Electromagnetic waves; Magnetic composite; Ferromagnetic materials; Microwaves

1. Introduction

Although electrical equipment provides convenience in our lives, the resulting EM radiation leads to pollution of the environment and harm to human beings. Therefore, the need to protect people or devices from harm and to keep a device from being detected by other instruments is leading to the development of novel EM-waves-absorbing materials [1–6]. The ideal EM wave absorber should possess light weight, high EM-wave absorption and multi-functionality [7–9].

Ferrites exhibit substantial magnetic losses in the vicinity of their natural resonance (FMR). Because of this they are one of the best materials for EM wave absorbers. Ferrites with a spinel crystal structure can be applied in the frequency range from several hundred MHz to several GHz [10]. AM_2O_4 spinel ferrites are binary ferromagnetic oxides from the system Fe_2O_3–MO, where M is usually a transition-metal element. Almost any divalent transition-metal ion can be used to form a spinel ferrite. The magnetic properties of ferrites can be considered in terms of the Neèl model of ferrimagnetism. One of the attractive properties of ferrites is the possibility to prepare different compositions and thereby modify the magnetic properties.

By varying the chemical composition it is possible to control the electromagnetic properties, such as the saturation magnetization, the magnetocrystalline anisotropy, the permeability and the permittivity of a ferrite composite. In addition, the microstructure of the ferrites has an additional impact on their properties, and consequently on the EM-wave absorption.

In general, EM-wave absorbers can be prepared in the form of ceramics or as composites, where the ceramic phases are embedded in a polymeric matrix. Here, the EM properties of the composites can be very effectively tuned, simply by varying the volume fractions of the constituent filler phases.

In addition, a synergetic effect of the constituent phases' properties may also be observed in some composites. For this reason magnetic composites are interesting for radio-frequency and microwave-frequency applications [11,12]. Furthermore, during the development of suitable absorbers, their composition and processing are equally important. By using rheological

* Corresponding author. Tel.: +386 1 722 40 09; fax: +386 1 722 43 50.
E-mail address: branka.music@helios.si (B. Mušič).
[1] www.helios.si.

0272-8842/$36.00 © 2011 Elsevier Ltd and Techna Group S.r.l. All rights reserved.
doi:10.1016/j.ceramint.2011.11.037

tests we can simulate different processes and predict the influence on the properties of the material. The measurements can be used for changes in the formulations or to study the suitability of the raw material or the process control. Rheological measurements are helpful in the development of new products, giving a better understanding of the processes and an easier prediction of the final properties of the material. The use electromagnetic absorbers in a limited wave spectrum require a specific rheological behaviour, a high solids content and a high-thickness application. In this paper we will present the influence of ferrite particles with a spinel crystal structure on the magnetic and rheological properties of the organic resin solution and/or their EM-wave absorbing characteristics in the frequency range from 100 MHz to 10 GHz.

2. Experimental

Ferrite powder with a composition $Mn_{0.66}Zn_{0.27}Fe_{2.07}O_4$ was prepared with a solid-state reaction from the starting oxides Fe_2O_3, Mn_3O_4 and ZnO. The mixture of oxide powders was homogenized and calcined at 900 °C in air for 4 h. The calcined powder was then milled in a planetary steel ball (Fritsch, Pulverisette 7) with water as the milling medium. The average grain size of the ferrite powder after milling was 1 μm, as measured with a laser spectrometer (Cilas HR 850). The milled and dried powder was sintered in a computer-controlled furnace at a temperature of 1370 °C for 4 h. The sintered ferrite powder was milled in a planetary mill (Fritsch, Pulverisette 7) with steel balls for different milling times. The obtained ferrite powders were dried at 100 °C for 3 h and finally characterized with scanning electron microscopy (SEM) and X-ray diffractometry (XRD). In addition, the specific surface area (BET) and the average grain size (Cilas HR 850) for each ferrite powder sample were also measured.

Ferrite absorber composites were prepared by mixing the ferrite powder and an organic solution polymer of acrylic-resin-based putty with concentration ratios of 50:50, 75:25 and 90:10, by weight. The ferrite composite suspensions were dried at 50 °C and finally pressed in the appropriate forming tool. The samples were compacted to form a toroid with an outer dimension of 6 mm, an inner dimension of 3 mm and a height of 3 mm in order to fit well into an APC-7 coaxial sample holder. Both the relative complex permittivity ($\varepsilon_r = \varepsilon' - j\varepsilon''$) and the relative complex permeability ($\mu_r = \mu' - j\mu''$) of the samples were measured using an Anritsu 37269D vector network analyser in the frequency range from 100 MHz to 10 GHz. The permeability and the permittivity were calculated from the measured scattering parameters [4].

The rheological properties of the ferrite absorber composites were measured using a Rheometer Anton Paar MC 301 with a parallel-plate measuring system (with a gap of 0.5 mm). All the rheology tests were made in the linear viscoelastic range, i.e., non-destructive shear conditions, up to $5 \times 10^{-3}\%$ of deformation.

3. Results and discussion

3.1. Phase analysis and SEM morphology

Fig. 1 shows an X-ray diffractogram of an MnZn ferrite sample prepared using the ceramic processing technique described earlier. The diffraction peaks in the figure correspond to pure MnZn ferrite.

Table 1 shows the average particle size and the specific surface area (BET) of the ferrite powder samples S1–S3.

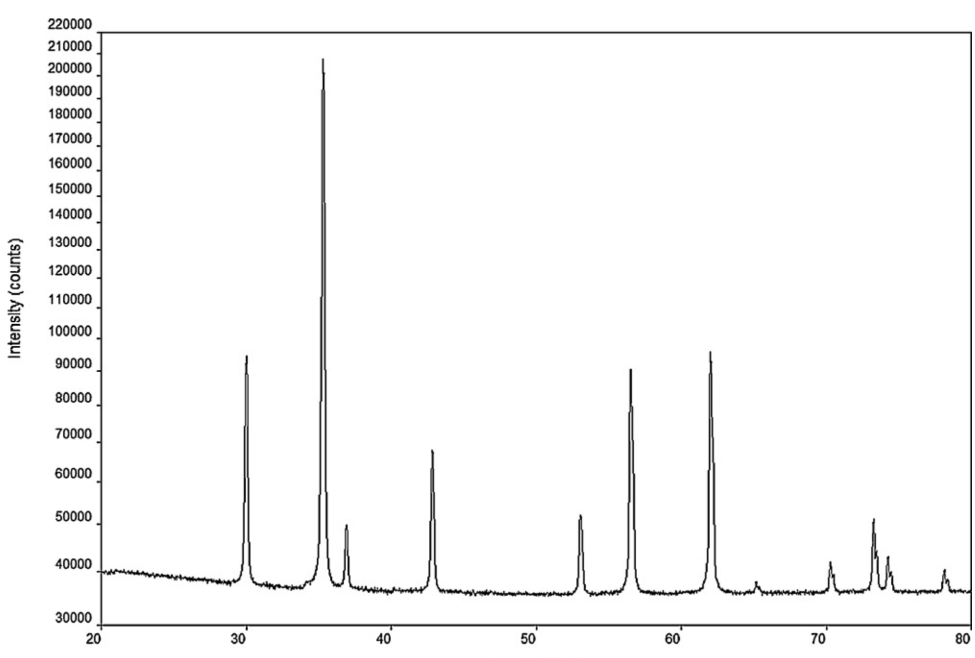

Fig. 1. X-ray diffractogram for MnZn ferrite prepared by ceramic processing.

Table 1
Specific surface area and average particle size for the samples S1–S3.

Sample code	Milling time (min)	Specific surface area (BET) (m^2/g)	Average particle size (μm)
S1	10	0.39 ± 0.01	14.95
S2	60	2.10 ± 0.02	4.24
S3	120	2.37 ± 0.02	3.70

Fig. 2(a)–(c) shows SEM images of MnZn ferrite particles after milling for the samples S1–S3. The powder obtained after the milling shows a wide particle size distribution, as seen in the SEM micrograph.

3.2. The relative complex permeability and permittivity

The complex permittivity ($\varepsilon_r = \varepsilon' - j\varepsilon''$) and complex permeability ($\mu_r = \mu' - j\mu''$) are known to determine the absorption characteristics of a material. The imaginary part of the permittivity and the imaginary part of the permeability of the composite specimens prepared for measurements of the absorbing characteristics in the frequency range from 100 MHz to 10 GHz with weight ratios of the ferrite powder to organic solution polymer of acrylic resin = 50:50, 75:25 and 90:10 were determined. The imaginary part of the permittivity and the imaginary part of the permeability of the composites with ferrite powders S1–S3 are presented in Figs. 3–5.

For the absorbing properties both the real and imaginary parts of the permittivity and the permeability are important; however, the imaginary part is directly associated with the losses. The electromagnetic properties of the ferrite composite mixtures are shown in Figs. 3–5. All the measured data were collected over a frequency range from 100 MHz to 10 GHz at room temperature. Figs. 3–5 show the imaginary part of the permeability for composites of ferrite powder S1–S3 with the weight ratios 50 wt.%, 75 wt.% and 90 wt.%. The figures indicate the significant influence of the ferrite powder's concentration on the imaginary part of the permeability and the imaginary part of the permittivity. Comparing the composite of ferrite powder S2 and the composite of ferrite powder S3, the composite of ferrite powder S3 showed higher maximum values in both the imaginary parts of the permeability and the imaginary parts of the permittivity. These lower values for the composite of the ferrite powder S3 are due to the different magneto-dynamic processes. Ferrite composites prepared using different concentrations of ferrite powders, 90 wt.%, 75 wt.% and 50 wt.%, respectively, showed a decrease of the imaginary permeability and permittivity with a decreasing concentration of ferrite powders, irrespectively of the particle size.

3.3. EM-wave absorption properties

According to the transmission-line theory, the reflection loss (RL) of electromagnetic radiation under normal wave incidence at the surface of a single/layer material backed by a perfect

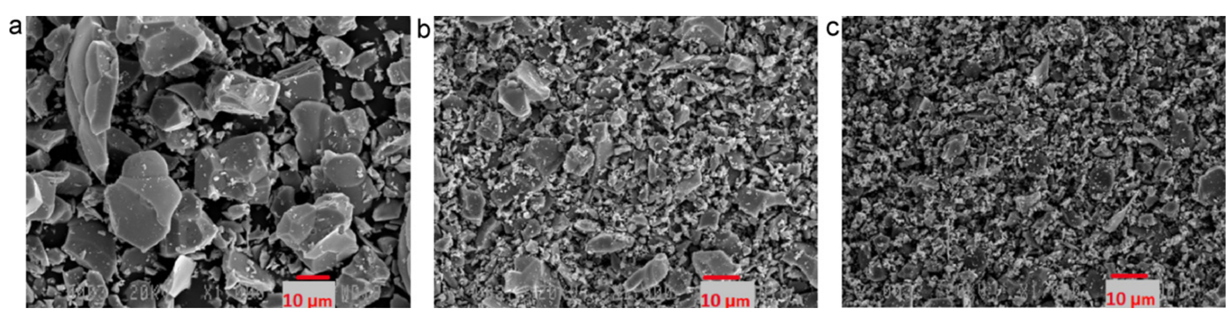

Fig. 2. SEM images of milled manganese zinc ferrite powder for samples S1 (a), S2 (b) and S3 (c).

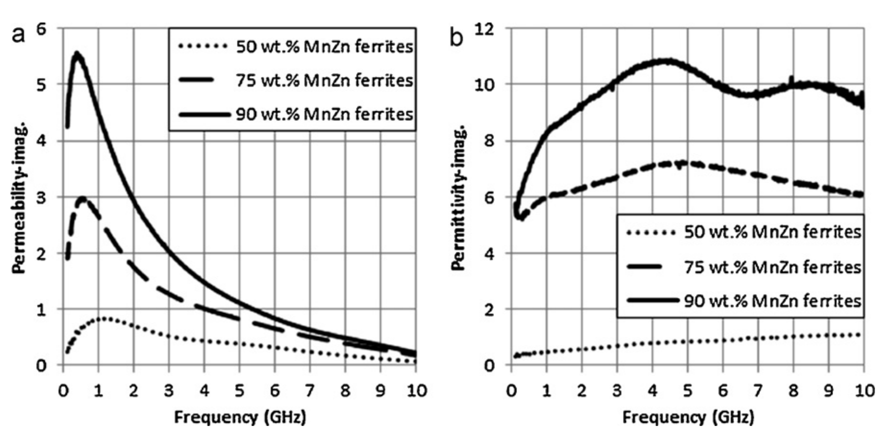

Fig. 3. The imaginary part of the permeability (a) and the imaginary part of the permittivity (b) for composite specimens with weight ratios of ferrite powder S1 to organic solution polymer of acrylic resin equal to 90:10, 75:25 and 50:50.

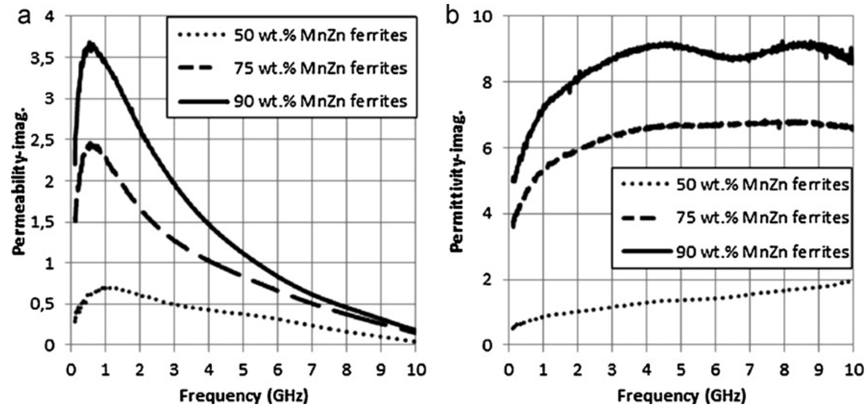

Fig. 4. The imaginary part of the permeability (a) and the imaginary part of the permittivity (b) of the composite specimens with weight ratios of ferrite powder S2 to organic solution polymer of acrylic resin equal to 90:10, 75:25 and 50:50.

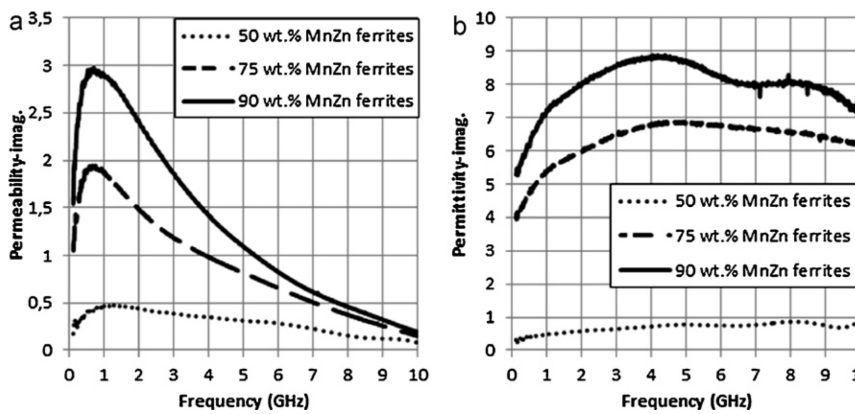

Fig. 5. The imaginary part of the permeability (a) and the imaginary parts of the permittivity (b) of composite specimens with weight ratios of ferrite powder S3 to organic solution polymer of acrylic resin equal to 90:10, 75:25 and 50:50.

conductor can be given by [9]

$$\mathrm{RL} = 20\log_{10}\left|\frac{Z_{\mathrm{in}} - Z_0}{Z_{\mathrm{in}} - Z_0}\right| \ \mathrm{dB} \tag{1}$$

where Z_0 is the characteristic impedance of free space,

$$Z_0 = \sqrt{\frac{\mu_0}{\varepsilon_0}} \tag{2}$$

and Z_{in} is the input impedance at the free space and material surface:

$$Z_{\mathrm{in}} = \sqrt{\frac{\mu_r}{\varepsilon_r}\tanh\left[j\left(\frac{2\pi t}{C}\right)\right]\sqrt{\mu_r\varepsilon_r}} \tag{3}$$

where μ_r and ε_r are the relative complex permeability and the permittivity of the composite medium, respectively, which can be calculated from the complex scatter parameter, where c is the velocity of light, f is the frequency of the incidence EW wave and t is the thickness of the composites. The impedance-matching condition is given by $Z_{\mathrm{in}} = Z_0$, representing the ideal absorbing conditions.

Figs. 6–8 show the dependence of the thickness of the absorber layer (d) on the reflection loss of the composite specimens with the weight ratio of the ferrite powder S1–S3 to organic solution polymer of acrylic resin being 75:25. The absorber layer (d) was 3-mm, 4-mm and 5-mm thick. It is clear that the average particle size of the ferrite powder has no influence on the reflection-loss peak, but shifted the frequency range. This shows that by changing the thickness of the material

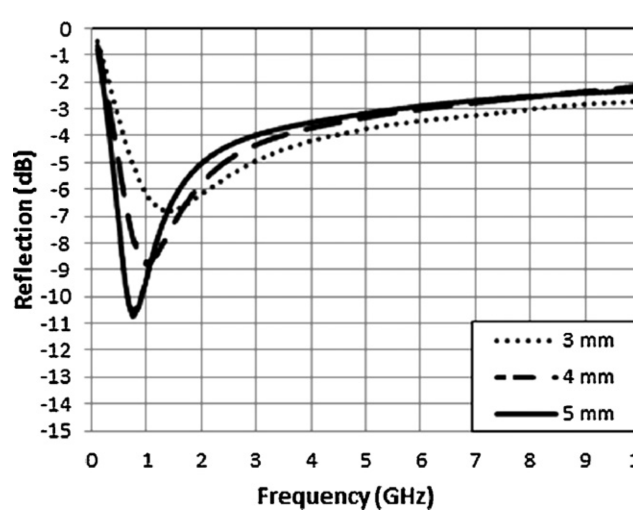

Fig. 6. The dependence of the thickness of the absorber layer d (3 mm, 4 mm and 5 mm) on the reflection loss of the composite specimens with the ferrite powder S1.

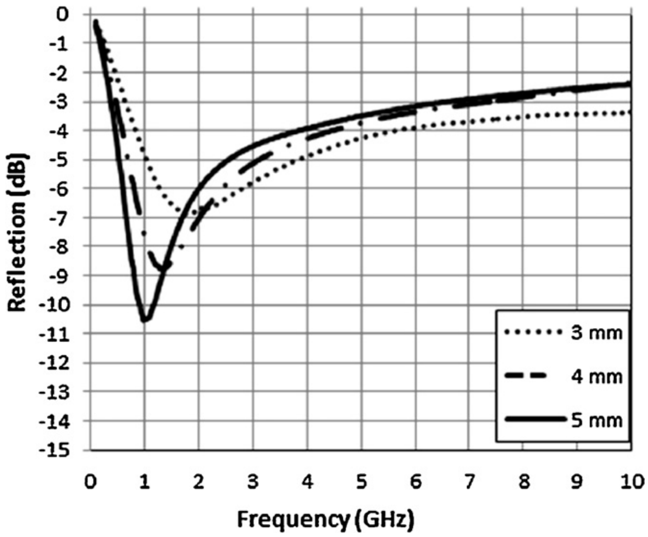

Fig. 7. The dependence of the thickness of the absorber layer d (3 mm, 4 mm and 5 mm) on the reflection loss of the composite specimens with the ferrite powder S2.

with the spinel structure the position and the attenuation-peak frequency can be easily manipulated in terms of the frequency range. We concluded that composite materials with a large fraction of the spinel phase/structure can be used as electromagnetic wave absorbers in the lower GHz range.

Figs. 6–8 show the variations of the reflection loss versus the frequency determined from the composite samples with filler phases S1–S3 and three sample thicknesses. The electromagnetic-wave absorption data in Figs. 6–8 are summarized in Table 2. Here, the bandwidth is defined as the frequency width in which the reflection loss is less than −10 dB, which indicates that 90 wt.% of the EM waves are absorbed by the material [8]. RL values of less than −10 dB were obtained with an absorber layer of $d = 5$ mm in the case of a composite with filler phases S1–S3.

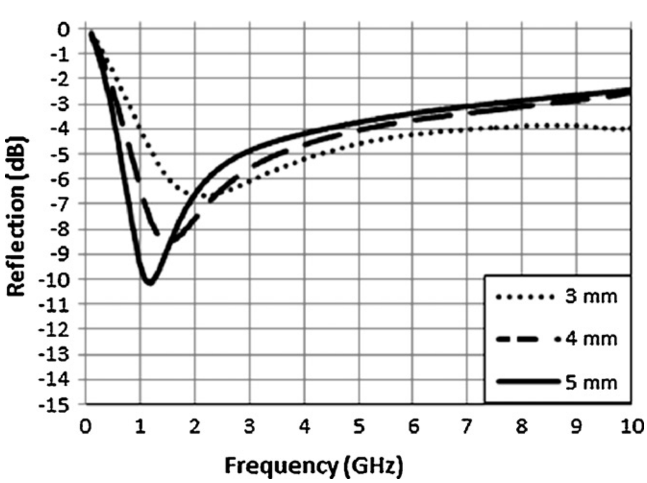

Fig. 8. The dependence of the thickness of the absorber layer d (3 mm, 4 mm and 5 mm) on the reflection loss of the composite specimens with the ferrite powder S3.

Table 2
Electromagnetic-wave absorption properties of composite samples.

Samples code	Thickness (mm)	Minimum RL fm (GHz)	Minimum RL value (dB)
S1	3	1.35	−6.81
	4	0.97	−8.78
	5	0.75	−10.73
S2	3	1.76	−6.88
	4	1.33	−8.78
	5	0.97	−10.53
S3	3	2.09	−6.72
	4	1.55	−8.5
	5	1.17	−10.17

3.4. Rheological properties

A rheological characterization of the magnetic materials provides important information for researchers who wish to improve and optimize their products and manufacturing processes [13]. Most materials are visco-elastic, which means that they show viscous and elastic behaviour. These properties can be determined by making dynamic measurements with oscillatory tests in the linear visco-elastic range, independent of the present strain [14]. All the rheology tests were made in the linear viscoelastic range.

For the test with a controlled shear stress as a sine function we obtained the $y(t)$ curve as a phase-shifted sine function

$$y(t) = y_0 \sin(\omega t + \delta) \quad (4)$$

The sine curve of the measured response is shifted by the angle δ ($0^\circ < \delta < 90^\circ$) compared to the present sine curve.

For an interpretation of the rheological properties we have two important parameters, i.e., G' and G''. The storage modulus G' [Pa] is a measure of the deformation energy stored in the sample during the shear process and represents the elastic behaviour of the sample. After the load is removed the storage energy is partially or completely compensated, like reversible deformation behaviour. The loss modulus G'' [Pa] is a measure of the deformation energy used up in the sample during the shear process and lost to the sample afterwards. It represents the viscous behaviour of the sample. This energy is either used up during the process of changing the sample's structure or dissipated into the surrounding environment in the form of heat.

$$\tan\delta = \frac{G''}{G'} \quad (5)$$

The ideal elastic behaviour is expressed as $\delta = 0^\circ$ and G' completely dominates G''. The ideal viscous behaviour is expressed as $\delta = 90^\circ$ and G'' completely dominates G'.

The ferrite particle sizes have a significant influence on the rheological behaviour of the magnetic composites.

In order to improve the application behaviour of the coatings, quite often the most important rheological information is the described time-dependent Oscillatory Three Step Tests. This characterization is important for the workability and application process of coatings, like the flow resistance or spreading. The course of the oscillatory 3 step test is as follows:

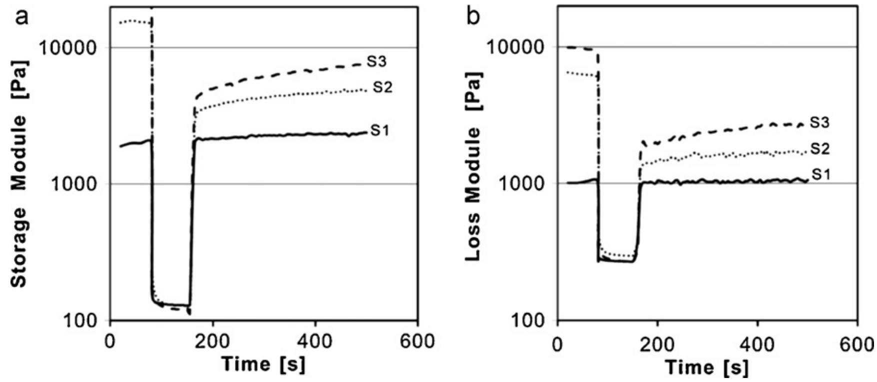

Fig. 9. The storage module (a) and loss module (b) of composite specimens with 75 wt.% of ferrite powder S1–S3, respectively, to organic solution polymer of acrylic resin.

step (1) rest phase under low-shear conditions (within the linear visco-elastic range) during the time period 0–80 s; step (2) load phase under high-shear conditions (outside the linear visco-elastic range) during the time period 80–250 s in order to decompose the sample structure; step (3) phase after removing the load (within the linear visco-elastic range) during the time period 150–500 s, under the same shear conditions as in the first interval, to facilitate the regeneration of the structures.

In Fig. 9 we can see that all the measured samples we have in the first and the third step storage modules (G') are higher than the Loss Modules (G''), which means that the samples have the character of a visco-elastic gel (sagging can be prevented and remixing of the components of the composite can be prevented). During the second step the samples have $G'' > G'$, which means that the samples have a liquid character (this shows good spreading). After removing the load under low-shear conditions the phases have, in the cases with particles S2 and S3, poor regeneration of the structure. The coatings with this characteristic can run away from the substrate. We can see this in the large differences between the values in the first and third steps.

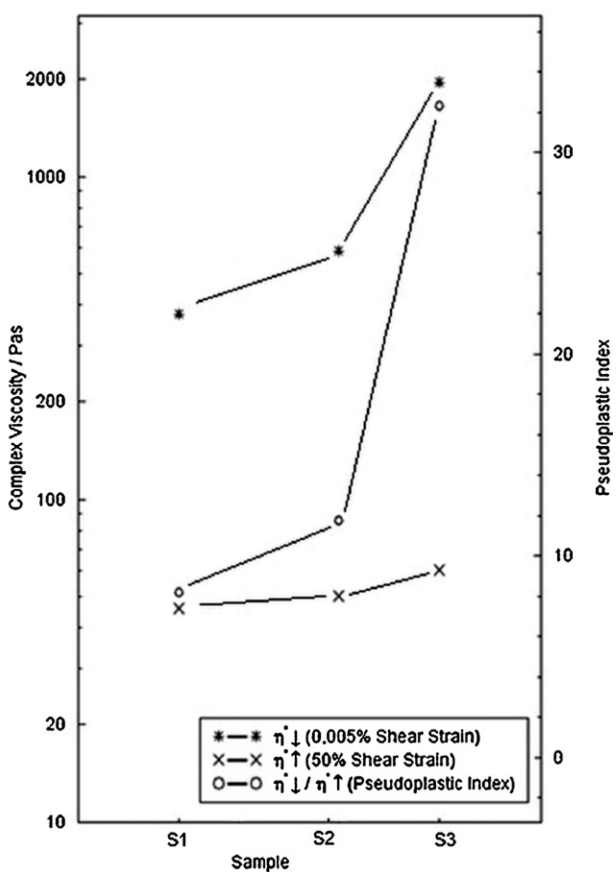

Fig. 10. Complex viscosities at lower and higher deformations and the pseudo-plastic indexes of the composite specimens with the ferrite powders S1–S3; reading at 450 s from the oscillatory 3rd step.

From the complex viscosity ($\eta^* \downarrow$) at the lower deformation (0.005%) and the complex viscosity ($\eta^* \uparrow$) at the higher deformation (50%) at the same frequency (1 Hz) we can calculate the pseudo-plastic indexes ($\eta^* \uparrow / \eta^* \downarrow$) for the samples under investigation (Fig. 10).

Fig. 10 shows the complex viscosity and the pseudo-plastic index of composite specimens in the organic solution polymer of acrylic resin with the weight ratio of ferrite powders (S1–S3) equal to 75%.

It is clear that the pseudo-plastic index in the case of sample S3 with a particle size of 3.70 μm is the greatest on account of large change in the complex viscosity value at low deformation. This effect is usually reflected in poor spreading.

4. Conclusion

The purpose of this study was the synthesis of the defined MnZn ferrites powders S1–S3 and an investigation of the electromagnetic absorber properties of resin compacts containing synthesized pure manganese zinc ferrites powders with well-defined particle sizes and surface areas.

The incorporation of electromagnetic absorber materials into organic polymer solutions of acrylic resin for use as architectural putty is a complex process because of the MnZn ferrites' large weight and the need for a high concentration of MnZn ferrites for efficient EM-absorbing properties. Besides a study of the efficiency of the EM absorption over a wide frequency range as a function of absorber–material concentration and particle size we investigated the influence of the required thickness of putty-coating, which is reflected in the rheology.

The particle size of the absorber ferrite powder has only a minor influence on the electromagnetic absorber properties, thus samples S1–S3 have a similar reflection of electromagnetic radiation in the case when we have the same concentration of ferrite powder and the same thicknesses of applied putty. However, the concentration of MnZn ferrite powders in the finally prepared putty has an influence on the highly efficient electromagnetic absorber properties.

The coatings, which have a complex structure, need to be characterized in terms of their structures and flow properties in order to be successfully applied. The high weight of the putty can lead to sliding from a vertical wall after it is applied. We determined that with a different particle size we can influence the rheology of the final putty. With a smaller particle size of the magnetic powders, like in the case of sample S3, we have higher visco-elastic properties and with larger powder particle sizes we have faster regeneration of the structure than in the case of sample S1. The S1 and S2 samples show good spreading and non-sagging properties.

The results of the study show that the incorporation of MnZn ferrite powder material into an organic polymer of acrylic resin can provide efficient EM absorption.

Acknowledgments

Operation part financed by the European Union, European Social Fund. Operation implemented in the framework of the Operational Programme for Human Resources Development for the Period 2007–2013, Priority axis 1: Promoting entrepreneurship and adaptability, Main type of activity 1.1.: Experts and researchers for competitive enterprises.

References

[1] S. Kim, D. Han, S. Cho, Microwave absorbing properties of sintered Ni–Zn ferrite, IEEE Trans. Magn. 30 (1994) 4554–4556.

[2] F.M.M. Pereira, M.R.P. Santos, R.S.T.M. Sohn, J.S. Almeida, A.M.L. Medeiros, M.M. Costa, A.S.B. Sombra, Magnetic and dielectric properties of the M-type barium strontium hex ferrite ($Ba_xSr_{1-x}Fe_{12}O_{19}$) in the RF and microwave (MW) frequency range, J. Mater. Sci.: Mater. Electron. 20 (2009) 408–417.

[3] A. Verma, R.G. Mendiratta, T.C. Goel, D.C. Dube, Microwave studies on strontium ferrite based absorbers, J. Electroceram. 8 (2002) 203–208.

[4] V.B. Bregar, D. Lisjak, A. Žnidaršič, M. Drofenik, The application of effective-medium theory for the nondestructive characterization of ceramic composites, J. Eur. Ceram. Soc. 27 (2007) 1071–1076.

[5] A. Ghasemi, A. Hossienpour, A. Morisako, X. Liu, A. Ashrafizadeh, Investigation of the microwave absorptive behavior of doped barium ferrites, Mater. Des. 29 (2008) 112–117.

[6] C.C. Chang, Y.C. Chen, G.P. Wang, C.C. Hwang, C.C. Yeh, Synthesis of nanocrystalline $SrFe_{12}O_{19}$ particles doped with $SrTiO_3$ via combustion synthesis for microwave absorption applications, J. Chin. Chem. Soc. 57 (2010) 976–981.

[7] Y.B. Feng, T. Qiu, C.Y. Shen, Absorbing properties and structural design of microwave absorbers based on carbonyl iron and barium ferrite, J. Magn. Magn. Mater. 318 (2007) 8–13.

[8] J. Huo, L. Wang, H. Yu, Polymeric nanocomposites for electromagnetic wave absorption, J. Mater. Sci. 44 (2009) 3917–3927.

[9] V.B. Bregar, A. Žnidaršič, Analysis of electromagnetic noise suppression in microstrip lines with absorber sheets, in: Proceedings. [S.I.]: Institute of Electronics, Information and Communication Engineers, Asia-Pacific Microwave Conference (2006) 12-15, Yokohama, Japan, (2006), pp. 540–543.

[10] M. Pardavi-Horvath, Microwave application of soft ferrites, J. Magn. Magn. Mater. 171 (2000) 215–216.

[11] T. Nakamura, E. Hankui, Control of high-frequency permeability in polycrystalline (Ba,Co)-Z-type hexagonal ferrite, J. Magn. Magn. Mater. 257 (2003) 158–164.

[12] F.M.M. Pereira, M.R.P. Santos, R.S.T.M. Sohn, J.S. Almeida, A.M.L. Medeiros, M.M. Costa, A.S.B. Sombra, Magnetic and dielectric properties of the M-type barium strontium hexaferrite ($Ba_xSr_{1-x}Fe_{12}O_{19}$) in the RF and microwave (MW) frequency range, J. Mater. Sci.: Mater. Electron. 20 (2009) 408–417.

[13] T.G. Mezger, The Rheology-Handbook, Vincentz Verlag, Hannover, 2002, pp. 16–65.

[14] G. Schramm, A Practical Approach to Rheology and Rheometry, Thermo Electron Karlsruhe, 2004, pp. 3–26.